JOURNAL OF AIRCRAFT
Vol. 38, No. 5, September–October 2001

Engineering Notes

ENGINEERING NOTES are short manuscripts describing new developments or important results of a preliminary nature. These Notes cannot exceed 6 manuscript pages and 3 figures; a page of text may be substituted for a figure and vice versa. After informal review by the editors, they may be published within a few months of the date of receipt. Style requirements are the same as for regular contributions (see inside back cover).

Altitude- and Weight-Scaling Laws for Ram-Air Parachute Inflation

J. Potvin*
Saint Louis University, St. Louis, Missouri 63103

Introduction

FOR decades parachute designers have used inflation scaling laws relating inflation time and opening shock to many deployment conditions and construction characteristics.[1–9] Most of these laws, however, are relevant only to the basic circular parachute, with or without geometric porosity, and without opening shock control devices. In this Note new inflation scaling laws on the effects of altitude and payload weight on the more modern ram-air parachute wings (or parafoils) are formulated and discussed. This analysis is a sequel to the numerical and experimental studies by Potvin[10] and by Potvin et al.[11] on the inflation of parafoils outfitted with an opening shock control device called the slider. These authors have also discussed the inflation scaling properties of ram-air parachutes but only with regard to changes of the canopy spreading rate constant and overall size.

Ram-Air Parachute Inflation and Ideal Parachute Model Scaling

Most modern parachutes use opening shock control devices in order to widen their deployment envelope. Ram-air parachutes are no exception, given their potential to open very quickly and hard if the spreading rate of the canopy is not slowed down. One such opening shock control device is the slider, which is used on a wide variety of parafoils[1,11] as well as on a few conventional round parachutes.[12–14] By design, slider-reefed parachutes deploy and inflate in four stages: 1) suspension line deployment and line stretch, 2) extraction of the parachute out of the bag, 3) early pressurization/partial inflation, and 4) full canopy spreading/slider descent.

The scaling laws discussed next are based on the Ideal Parachute Model (IPM), which is designed for the simulation of slider-reefed ram-air parachutes inflating along a purely vertical trajectory.[10] The IPM is a non-Computational-fluid-dynamics approach to the study of inflation, being based on the simultaneous solution of the equation of motions of the payload and of the slider. The study by Potvin et al.[11] discusses its validation with data collected on dozens of manned, instrumented jumps. Comparison between model and experimental data for canopies of up to 200 ft^2 surface area has shown good agreement. Because the IPM describes only the full canopy spreading stage, maximum opening forces are accurately calculated only for those canopies that experience opening shock during that stage.

The scaling laws formulated in Refs. 10 and 11 were obtained from IPM simulations corresponding to thousands of different parachute component sizes, deployment speeds, and deployment altitudes. The most interesting features of these runs were the scaling of the payload maximum deceleration $a_{\max}$ and time of maximum deceleration $t_{\max}$, which turn out to depend on only one dimensionless ratio[10,11]:

$$a_{\max}/g = 0.360R_p^{0.332} \qquad t_{\max}g/V_0 = 1.532R_p^{-0.354} \tag{1}$$

Here $R_p = \rho K V_0^6/2Wg^2$ and parameters V_0, W, g, and ρ correspond to the payload's descent rate at the onset of full canopy spreading, the combined weight of the parachute and payload, the constant of gravity and the air density at deployment/inflation altitude, respectively. The dimensionless constant K describes the opening rate of the instant canopy drag area $C_D(t)S(t)$ and is defined by[10] $d^2[C_D(t)S(t)]/dt^2 = KV(t)^2$. It is sufficient to know that K is proportional to a combination of air density, parachute's average drag coefficient C_D^{aver} over entire inflation sequence, slider mass m_{slider}, suspension line length $L_{\text{susp line}}$, wing chord L_{chord}, and span L_{span} (when fully inflated), namely $K \propto [C_D^{\text{aver}}\ \rho L_{\text{chord}}\ L_{\text{span}}\ C_D(0)S(0)]/(2m_{\text{slider}}\ L_{\text{susp line}})$. Not shown is the dependence of K on the difference of surface-area ratios between slider and main canopy, which has no bearing to the discussion at hand.[10,11] The scaling laws discussed next and in Ref. 11 are based on the scaling properties of ratio R_p, which happens to be expressible in terms of the more familiar Froude and mass ratio numbers as discussed next.

Because a parachute begins decelerating the payload as soon as it is deployed, the value of the descent speed at the onset of the canopy spreading stage V_0 is rarely equal to the speed at time of deployment. An estimate for V_0 is obtained by directly integrating the equation of motion for the case of a payload falling under a partly opened parachute of constant drag area $\Sigma_0 \equiv C_D(0)S(0)$ from an initial speed of V_{ff}, which is the payload's terminal freefall speed prior to parachute deployment. The resulting formula thus expresses V_0 in terms of the parachute-load system descent rate at the onset of deployment (i.e., V_{ff}), and of the duration of the early pressurization stage t_{ep} (Ref. 11):

$$V_0 = V_T\left(\frac{1 + Ae^{-V_T t_{\text{ep}}/D}}{-1 + Ae^{-V_T t_{\text{ep}}/D}}\right) \tag{2}$$

where $m = W/g$, $D = m/(\rho\Sigma_0)$, $A = (-V_{\text{ff}} + V_T)/(-V_{\text{ff}} - V_T)$ and $V_T^2 = 2\ W/(\rho\Sigma_0)$; moreover, $V_0 < 0$, $V_{\text{ff}} > 0$, and $V_T > 0$. Here V_T would correspond to the terminal fall speed of the payload when suspended under a partly opened canopy of fixed drag area Σ_0. Such drag area turns out to be that of the parachute during the early pressurization stage.

New Scaling Laws

Altitude Scaling

Knacke[1] points out the surprise caused by round parachute test drops carried out years ago at altitudes ranging between 2000 ft mean sea level (msl) and 40,000 ft msl in launch conditions characterized by a near-constant dynamic pressure $q = \frac{1}{2}\rho V^2$. On one hand, parachutes carrying very heavy payloads exhibited almost no change in opening shock, as the dynamic pressures at the various inflation stages remained similar those experienced at low altitude. Against all expectations, on the other hand, the opening shock of parachutes carrying light payloads was found to dramatically increase with

Received 19 April 2001; accepted for publication 1 May 2001.

*Associate Professor, Parks College Parachute Research Group, Department of Physics, 3450 Lindell Boulevard. Member AIAA.

altitude, in some cases by as much as 400% at 40,000 ft. Not much has been done theoretically to understand this phenomenon. Some measure of explanation can be obtained for the first time from the derivation of altitude scaling as prescribed by the IPM.

Scaling with respect to a change of air density can be expressed in terms of the factor Γ, a ratio of air densities at high and low altitudes ($\Gamma = \rho^{\text{high}}/\rho^{\text{low}}$), while keeping fixed all construction lengths, weight, and other parameters. The following equations, a summary of the air density scaling laws, show the ensuing Γ dependence for the variables used in Eqs. (1) and (2): $K^{\text{high}} = \Gamma K^{\text{low}}$, $V_T^{\text{high}} = \Gamma^{-1/2} V_T^{\text{low}}$, $V_{\text{ff}}^{\text{high}} = \Gamma^{-1/2} V_{\text{ff}}^{\text{low}}$, $A^{\text{high}} = \Gamma^0 A^{\text{low}}$, $D^{\text{high}} = \Gamma^{-1} D^{\text{low}}$, $t_{\text{ep}}^{\text{high}} = \Gamma^{1/2} t_{\text{ep}}^{\text{low}}$. For $\Gamma \ll 1$ and small t_{ep} $V_0^{\text{high}} \approx -\Gamma^{-1/2} V_{\text{ff}}^{\text{low}}$, $V_T^{\text{high}} = \Gamma^{-1/2} V_T^{\text{low}}$ $(a_{\max}^{\text{high}}/a_{\max}^{\text{low}}) \approx (\Gamma^{-1/3})$ $(-V_{\text{ff}}^{\text{low}}/V_0^{\text{low}})^{2.00}$ and $(t_{\max}^{\text{high}}/t_{\max}^{\text{low}}) \approx (\Gamma^{-0.146})$ $(-V_{\text{ff}}^{\text{low}}/V_0^{\text{low}})^{-1.124}$. These equations give the resulting scaling laws for $a_{\max}$ and $t_{\max}$ in the limit $\Gamma \ll 1$ and for small t_{ep}, i.e., $t_{\text{ep}} < 2$ s, a realistic range. A more accurate calculation can be performed at arbitrary t_{ep} and Γ, using a spreadsheet program together with the previous scaling identities. Not obvious is the scaling of the time of the early pressurization stage t_{ep}, which, according to the wind-tunnel study of Montanez et al.,[15] is calculated in terms of V_{ff}, the parachute wing chord, and the cell leading-edge inlet size through the equation $t_{\text{ep}} = (L_{\text{chord}}/V_{\text{ff}})\ (L_{\text{cellwidth}} L_{\text{cellheight}})^{0.5}/\delta$, where δ is a factor depending mostly on cell inlet design. This result implies the following relationship: $t_{\text{ep}}^{\text{high}} = \Gamma^{1/2}\ t_{\text{ep}}^{\text{low}}$.

The value of $a_{\max}$ increases with altitude as Γ decreases, being proportional to $\Gamma^{-1/3}$, and is modulated by the design and drop-specific ratio $(V_{\text{ff}}/V_0)^{\text{low}}$ measured at low altitude. On the other hand, the value of $t_{\max}$ increases or decreases depending on the relative values of Γ and $(V_{\text{ff}}/V_0)^{\text{low}}$. Typically, small parachutes carrying a heavy payload will be characterized by the least air density dependence, given the payload's high inertia causing almost no initial deceleration and leading to $V_0 \approx V_{\text{ff}}$. On the other hand, lightly loaded parachutes will feature the largest changes as $V_{\text{ff}} \gg V_0$. The altitude dependence of a specific canopy design can thus be manipulated by tuning the magnitude of V_0 through the duration of the early pressurization stage t_{ep} [see Eq. (2)]. Canopies with very short early pressurization duration would tend to open hard and be insensitive to altitude effects (because $V_0 \approx V_{\text{ff}}$). This would contrast with designs featuring a long early pressurization (where $V_{\text{ff}} \gg V_0$), which would open softly at low altitudes but open very hard at high altitudes. For example, using specific design parameters relevant to sport ram-air parachutes would involve values of the order of $W \sim 210$ lb, $\Sigma_0 \sim 10$ ft^2, $\Sigma_{\text{final}} \sim 150$ft^2, $t_{\text{ep}} \sim 1$ s, $v_{\text{ff}} \approx 176$ ft/s, $V_T \approx 135$ ft/s, $V_0 \approx -158$ ft/s, thus yielding at 40,000 ft an increase in maximum deceleration of the order of $a_{\max}^{\text{high}}/a_{\max}^{\text{low}} \sim 2.0$. This estimate is of the same order of magnitude as the existing data on the inflation of round personnel parachutes at high altitudes, but is somewhat smaller given that parafoils use inflation control hardware and old round parachutes do not.[1] In this example the time of maximum deceleration would increase, but only slightly so that $t_{\max}^{\text{high}}/t_{\max}^{\text{low}} \sim 1.09$.

The increase of parachute opening force with altitude can be understood by the fact that at low air densities opening speeds are greater but in a proportion that leads to a greater dynamic pressure. This can be seen by estimating the dynamic pressure at the onset of slider descent using the data of the air density scaling laws. Here one would have $\rho_{\text{high}}(V_0^{\text{high}})^2 = \rho_{\text{low}}(V_{\text{ff}}^{\text{low}})^2 > \rho_{\text{low}}(V_0^{\text{low}})^2$ because the ratio V_{ff}/V_0 is always greater than unity at any altitudes. In the case of the heavily loaded parachute, one would have $V_0 \approx V_{\text{ff}}$, which only leads to a small change of dynamic pressure.

Weight Scaling

The scaling properties of opening shock with respect to weight is another design law important to parachute developers, particularly in the skydiving industry where parachute size and jumper weight are scaled up or down from a well-tested prototype. Here a weight change factor γ is defined via $W_{\text{heavy}} = \gamma W_{\text{light}}$, while keeping fixed all construction lengths and deployment altitude. It is understood that the parachute's weight is negligible compared to that of the payload in order to be consistent with the constraint of fixed construction dimensions.

Weight scaling of each of the variables used in Eqs. (1) and (2) is shown here: $K^{\text{heavy}} = \gamma^0 K^{\text{light}}$, $V_T^{\text{heavy}} = \gamma^{1/2} V_T^{\text{light}}$, $V_{\text{ff}}^{\text{heavy}} = \gamma^{1/2} V_{\text{ff}}^{\text{light}}$, $A^{\text{heavy}} = \gamma^0 A^{\text{light}}$, $D^{\text{heavy}} = \gamma D^{\text{light}}$, $t_{\text{ep}}^{\text{heavy}} = \gamma^{-1/2} t_{\text{ep}}^{\text{light}}$. For $\gamma \to \infty$ and small t_{ep} $V_0^{\text{heavy}} \approx -\gamma^{1/2} V_{\text{ff}}^{\text{light}}$, $(a_{\max}^{\text{heavy}}/a_{\max}^{\text{light}}) \approx \gamma^{2/3}$ $(-V_{\text{ff}}^{\text{light}}/V_0^{\text{light}})^2$, $(t_{\max}^{\text{heavy}}/t_{\max}^{\text{light}}) \approx (\gamma^{-0.208})$ $(-V_{\text{ff}}^{\text{light}}/V_0^{\text{light}})^{-1.124}$. Again, the duration of the early pressurization stage is assumed to go as $t_{\text{ep}} \propto L_{\text{chord}}/v_{\text{ff}}$, therefore implying $t_{\text{ep}}^{\text{high}} = \gamma^{-1/2}\ t_{\text{ep}}^{\text{low}}$. As in the case of altitude scaling, the exact change of $a_{\max}$ and $t_{\max}$ can be computed using a spreadsheet program together with Eqs. (1) and (2) and the weight scaling laws just shown. In the regimes of large weight increases and small t_{ep}, the maximum deceleration increases with $\gamma^{2/3}$, while the time of maximum deceleration decreases or increases depending on the value of the ratio V_{ff}/V_0.

As with air density scaling, the design- and drop-specific ratio V_{ff}/V_0 may be the crucial factor for determining weight scaling for parachute designs characterized by $V_{\text{ff}} \gg V_0$, such as with canopies with long early pressurization times. For example, using the skydiving parachute design parameters already listed one arrives at an estimated $a_{\max}^{\text{heavy}}/a_{\max}^{\text{light}} \sim 1.97$ when the suspended weight is doubled. On the other hand, the time of maximum deceleration would decrease as $t_{\max}^{\text{heavy}}/t_{\max}^{\text{light}} \sim 0.77$.

Concluding Remarks

The altitude- and weight-scaling properties of ram-air parachutes show trends that are very similar to those of round parachutes. This can be seen by rewriting Eqs. (1) in terms of the well-known Froude number ($F_r \sim V^2/gS^{1/2}$) and mass-ratio number ($M_r \sim m/\rho S^{3/2}$), given that $R_p/K = [F_r(V_0)]^3/2M_r$. However, to be consistent with the analyses of Refs. 2, 3, 4 and 6, one needs to relate the value of the Froude number, here calculated at the moment of full canopy spreading, to its value at line stretch, namely $F_r(V_0) = (V_0/V_{\text{ff}})^2 F_r(V_{\text{ff}})$. Rewriting Eqs. (1) in these terms shows that highly loaded canopies characterized by $V_0 \sim V_{\text{ff}}$ feature opening shocks that are directly proportional to the Froude number at line stretch, in similarity with round-type parachutes.[2–4] Because $V_{\text{ff}}^2 \propto W$, these loaded canopies will show a moderate dependence on the mass ratio, namely $F_{\max} \propto W^{5/3} \propto M_r^{5/3}$, again in a manner consistent with round parachutes.[6]

Acknowledgments

The author acknowledges fruitful discussions with the following individuals: G. Peek and B. Brocato from the Parks College Parachute Research Group; W. Coe from Performance Designs, Inc.; S. Reid from Rigging Innovations, Inc; and G. Baumgartner, J. Olsen, J. Raudenbush, and G. Steele, from the U.S. Bureau of Land Management Smokejumpers.

References

[1] Knacke, T. W., *Parachute Recovery Systems Design Manual*; Para Publishing, Santa Barbara, CA, 1992.

[2] Lingard, J. S., "A Semi-Empirical Theory to Predict the Load-Time History of an Inflating Parachute," AIAA Paper 84-0814, April 1984.

[3] Lee, C. K., "Modeling of Parachute Opening: an Experimental Investigation," *Journal of Aircraft*, Vol. 26, No. 5, 1989, pp. 444–451.

[4] Lee, C. K., "Experimental Investigation of Full-Scale and Model Parachute Opening," AIAA Paper 84-0820, April 1984.

[5] Heinrich, H. G., and Hektner, T. R., "Flexibility as a Model Parachute Performance Parameter," *Journal of Aircraft*, Vol. 8, No. 5, 1971, pp. 704–709.

[6] Wolf, D., "Opening Shock," AIAA Paper 99-1702, June 1999.

[7] Niemi, E. E., "An Impulse Approach for Determining Parachute Opening Loads for Canopies of Varying Stiffness," AIAA Paper 91-0874, April 1991.

[8] Johari, H., and Desabrais, K. J., "Scaling for Solid Cloth Parachutes," AIAA Paper 2001-2007, May 2001.

[9] Berndt, R. J., and Deweese, J. H., "A Filling Time Prediction Approach for Solid Cloth Type Parachute Canopies," 2nd *AIAA Aerodynamic Decelerator Systems Technology Conference*, AIAA, Reston, VA, 1996, pp. 17–32.

[10] Potvin, J., "Testing a New Model of Ram-Air Parachute Inflation," *The Aeronautical Journal*, Vol. 101, 1997, pp. 299–313.

[11] Potvin, J., Peek, G., and Brocato, B., "Modeling the Inflation of Ram-Air

Parachutes Reefed with Sliders," *Journal of Aircraft*, Vol. 38, No. 4, 2001, pp. 818–827.

[12]Butler, M., and Crowe, M., "Design, Development and Testing of Parachutes Using the BAT Sombrero Slider," AIAA Paper 99-1708, June 1999.

[13]Potvin, J., Peek, G., Brocato, B., Perschbacher, T., and Kutz, R., "Inflation and Glide Studies of Slider-Reefed Cruciform Parachutes," AIAA Paper 2001–2021, May 2001.

[14]Richards, F. H., and Buckley, J., "Developmental Efforts of the Dual-Mode Recovery System for Integration into the Navy's System Seat Demonstrator," *Proceedings of the 32nd Annual SAFE Symposium*, 1994, pp. 164–174.

[15]Montanez, R., Potvin, J., and Peek, G., "Wind Tunnel Investigation of Ram-Air Parachute Cell Pressurization," AIAA Paper 97-1524, June 1997.

Aeroservoelastic Design Optimization with Experimental Verification

Dan Borglund*
Kungliga Tekniska Högskolan, SE-10044 Stockholm, Sweden

Introduction

In optimal design of structures subject to fluid-dynamic forces, the most common objective is to minimize the structural weight subject to constraints on structural stability. A recent example in aircraft structures is Eastep et al.[1] As stressed by Kuttenkeuler and Ringertz,[2] the use of optimal design methods tends to increase the likelihood of obtaining structures that are extremely sensitive to imperfections. As a consequence, possible interactions with for example a control system can have severe effects on the structural performance if not accounted for in the structural design optimization.

In aeroservoelasticity, significant efforts have been devoted to the use of active control systems to stabilize flexible aircraft structures. In particular, wing flutter suppression using aerodynamic control surfaces has been successfully demonstrated in wind-tunnel experiments, see, for example, Ghiringhelli et al.[3] However, in most such active control design the objective is to improve the performance of a structure designed without consideration of the control system.

A previous study[4] focusing on structures with internal pipe flow has indicated that significant improvements are possible in terms of reduced structural weight and control system performance by integrating the design of the control system in a structural design optimization. An integrated design optimization was performed, where the structural weight was minimized using both structural dimensions and control system parameters as design variables. In this Note the same approach is applied to the system of a cantilever flexible wing subject to unsteady aerodynamic loads.

Experimental Setup

A schematic layout of the wind-tunnel experimental setup is shown in Fig. 1. A rectangular flexible wing with semispan 1.2 m and aspect ratio 10 was mounted vertically in a low-speed wind tunnel at Kungliga Tekniska Högskolan. An electric servo was used for digital control of an aileron having approximately one-fourth the dimensions of the wing. To reduce the finite-span effects not accounted for in the numerical model (see "Aeroservoelastic Analysis"), the wing was equipped with vertical winglets as shown in Fig. 1. A detailed description of the wing geometry, structural properties, actuator performance, and the digital control system can be found in Borglund and Kuttenkeuler.[5] The environmental conditions were room temperature and atmospheric pressure in all wind-tunnel tests. Hence, standard atmospheric conditions is used in the subsequent analysis of the wing.

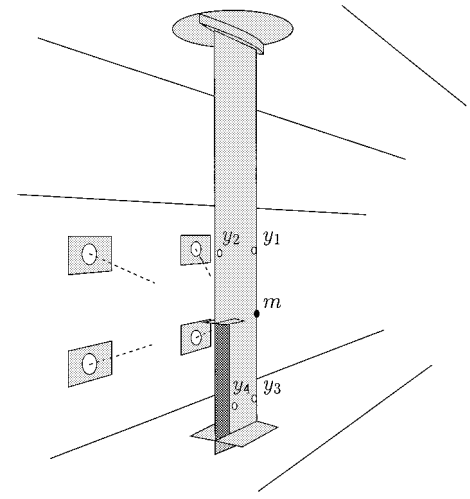

Fig. 1 Schematic layout of the wind-tunnel experiment.

The elastic deformation of the wing was monitored by a noncontact optical measurement system, capable of real-time three-dimensional tracking of reflecting markers attached to the wing. The optical system is based on four charge-coupled device cameras mounted in the wind-tunnel walls (see Fig. 1). Sufficient observability of the dominant aeroelastic modeshapes was achieved by placing two markers (y_1 and y_2) at midwing leading- and trailing-edge positions and another pair (y_3 and y_4) closer to the wing tip. Thus, the output to be used for feedback control of the wing is the four wing displacements y_1–y_4, measured by the optical system. For more details on the optical system, the reader is referred to Kuttenkeuler.[6]

Aeroservoelastic Analysis

Using beam theory for the structural dynamics, strip theory for the unsteady aerodynamic loads, and discretizing using beam finite elements,[5] the equations of motion for small elastic deformations of the wing can be written in the form

$$\dot{\boldsymbol{w}} = \boldsymbol{Q}(k, u)\boldsymbol{w} + \boldsymbol{q}\delta \tag{1}$$

$$\boldsymbol{y} = \boldsymbol{C}\boldsymbol{w} \tag{2}$$

where the dot denotes differentiation with respect to time t. The state vector $\boldsymbol{w}(t)$ is composed of aeroelastic states, actuator states, and states corresponding to approximations of time delays in the digital control system. The system matrix $\boldsymbol{Q}(k, u)$ is complex nonsymmetric and depends on the airspeed u and the reduced frequency $k = \omega b/u$, where w is the frequency of vibration and b the wing semichord. The setpoint for the aileron deflection is denoted $\delta(t)$, which enters the state equation through the input vector $\boldsymbol{q}$. The measured wing displacements $\boldsymbol{y}(t) = [y_1 \;\; y_2 \;\; y_3 \;\; y_4]^T$ are extracted from the aeroelastic states by the output matrix $\boldsymbol{C}$.

A simple output feedback controller is defined by

$$\delta = \boldsymbol{k}^T(u)\boldsymbol{y} \tag{3}$$

where $\boldsymbol{k}(u)$ is a vector of four feedback gains, which are allowed to depend on the airspeed. Inserting Eqs. (3) and (2) into (1) and transforming to the frequency domain using $\boldsymbol{w}(t) = \hat{\boldsymbol{w}}e^{pt}$ gives the nonlinear eigenvalue problem

$$\{\boldsymbol{I}\hat{p} - (b/u)[\boldsymbol{Q}(k, u) + \boldsymbol{q}\boldsymbol{k}^T(u)\boldsymbol{C}]\}\hat{\boldsymbol{w}} = \boldsymbol{0} \tag{4}$$

where the reduced closed-loop pole (eigenvalue) $\hat{p} = pb/u$ has been introduced for convenience. The nonlinearity is caused by the dependence on the reduced frequency of oscillation $k = \omega b/u$, which is the imaginary part of $\hat{p}$. For a given airspeed u and control law $\boldsymbol{k}(u)$ the eigenvalue problem (4) is solved iteratively using the so-called

Received 22 August 2000; presented as Paper 2000-4829 at the AIAA/USAF/NASA/ISSMO 8th Symposium on MDO, Long Beach, CA, 6–8 September 2000; revision received 20 June 2001; accepted for publication 25 June 2001.

*Research Associate, Department of Aeronautics. Member AIAA.